

Chandra Resolves the Double FU Orionis System RNO 1B/1C in X-rays

STEPHEN L. SKINNER¹ AND MANUEL GÜDEL²

¹*Center for Astrophysics and Space Astronomy (CASA), Univ. of Colorado, Boulder, CO, USA 80309-0389*

²*Dept. of Astrophysics, Univ. of Vienna, Türkenschanzstr. 17, A-1180 Vienna, Austria*

Submitted to AJ (in press)

ABSTRACT

We present new *Chandra* X-ray observations of the close pair of young stars RNO 1B and 1C (6'' separation) located in the L1287 cloud. RNO 1B erupted in 1978 - 1990 and is classified as an FU Orionis star (FUor). RNO 1C also shows most of the properties of an FUor but no eruption has yet been seen. Only a few dozen FUors are known and the presence of two such objects with a small angular separation is rare, suggesting a common origin. Both stars were faintly detected by *Chandra* and we summarize their X-ray properties within the framework of other previously detected FUors. We also report other X-ray detections in L1287 including the deeply-embedded young star RNO 1G, the jet-like radio source VLA 3, and an enigmatic hard flaring source with no 2MASS counterpart that was only detected in the second of two *Chandra* exposures.

Keywords: stars: individual (RNO 1B/1C) — stars: pre-main-sequence — X-rays: stars

1. INTRODUCTION

FUors are low-mass pre-main sequence (PMS) stars which undergo large optical or IR outbursts of several magnitudes followed by a slow decay on timescales of decades or longer. The prototype FU Ori erupted optically in 1936-37 and is still in slow decline. The outbursts are thought to be due to a dramatic increase in the accretion rate from the circumstellar disk onto the star. The enhanced accretion is accompanied by development of a strong cool wind. FUors also show wavelength-dependent spectral types mimicing low surface gravity F-G giants or supergiants in the optical (attributed to a self-luminous accretion disk), infrared excesses, and 2.3 μ m CO absorption.

Only about two dozen FUors are known (Audard et al. 2014; Connelley & Reipurth 2018, hereafter CR18). It is thus quite remarkable that a close pair of such objects, RNO 1B and 1C (6'' separation) exists in the L1287 cloud. At the L1287 distance of 929 ± 34 pc (Reid et al. 2014), their separation is ≈ 5574 AU. The two stars probably formed contemporaneously and it has been suggested that both 1B and 1C may be close binaries, comprising a hierarchical quadruple system (Reipurth & Aspin 2004).

The L1287 region contains RNO 1, which was listed in the catalog of red and/or nebulous objects (RNO) compiled by Cohen (1980). Subsequently, Staude & Neckel (1991, hereafter SN91) obtained *I*-band images which resolved the nebulous RNO 1 region into several compact knots including the close pair RNO 1B and 1C, now known to be young stars (Kenyon et al. 1993). They have similar 2MASS K_s magnitudes of $K_s = 7.76$ (1B) and $K_s = 7.54$ (1C). Both are viewed through high extinction. Estimates for RNO 1B are $A_V \approx 9.2$ mag (SN91) to 14.5 ± 1 mag (CR18). RNO 1C is redder with $A_V \approx 12$ mag (SN91) to 19.5 ± 4 mag (CR18). RNO 1B (= V710 Cas) brightened by at least 3 mag in *R* band between 1978 - 1990 (SN91) and is a classical (outburst) FUor. No eruption has yet been seen in RNO 1C but it does show most of the defining features of the class, so it is classified as FUor-like (CR18; Kenyon et al. 1993).

We report the first X-ray detection of RNO 1B and 1C. Our main objective was to use *Chandra*'s excellent spatial resolution to resolve the pair and quantify their X-ray properties, placing them into context with other X-ray detected FUors such as FU Ori (Skinner et al. 2006; 2010) and the classical FUor V1735 Cyg (Skinner et al. 2009).

2. OBSERVATIONS

We observed RNO 1B/1C with the *Chandra* Advanced CCD Imaging Spectrometer (ACIS-I) in two separate exposures on 2018 Mar 20 (ObsId 20135; 34.507 ks live-

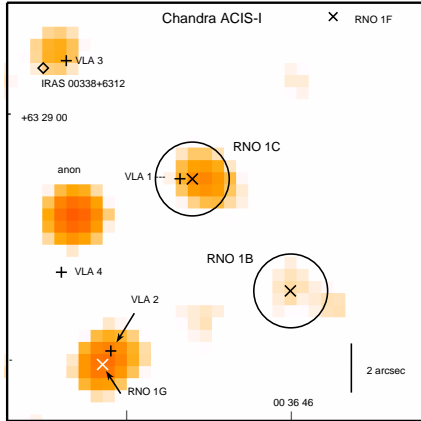


Figure 1. *Chandra* ACIS-I image (0.5-7 keV; log intensity scale) of the region near RNO 1B/C based on merged event data from ObsIds 20135 and 21041 (59.143 ks). The image has been lightly Gaussian smoothed using a 3-pixel kernel to bring out faint emission from RNO 1B (5 counts) and 1C (8 counts). The 2MASS positions (×) and $r=1''.5$ source extraction regions of RNO 1B and 1C are shown. The position of RNO 1G (×) is from Quanz et al. (2007). VLA radio positions (+) are from Anglada et al. (1994). The source labeled “anon” is CXO J003647.3+632856. Sources RNO 1F and VLA 4 were not detected by *Chandra*.

time) and 2018 May 29 (ObsId 21041; 24.636 ks) providing a total livetime of 59.143 ks. The ACIS detector is sensitive in the $E \approx 0.4$ -10 keV energy range with a pixel size of $0''.492$. For on-axis sources, 90% of the encircled energy fraction (EEF) lies within a radius of $R_{90} \approx 0''.9$ at $E=1$ keV. The EEF is energy-dependent and R_{90} increases toward higher energies¹.

Data were reduced using standard threads in the *Chandra* Interactive Analysis of Observations (CIAO v4.11) package. Events from the two exposures were reprojected onto the same tangent point and merged using the CIAO *merge_obs* script. The image created from the merged events is shown in Figure 1. For sources of interest, spectra and associated response files were extracted separately for each observation and then fitted simultaneously using *XSPEC* v. 12.10.1.

3. RESULTS

3.1. RNO 1B and 1C

Table 1 summarizes the X-ray properties of RNO 1B and 1C and other sources in their vicinity. For RNO 1B, the summed exposures yielded 5 events inside a $r=1''.5$ extraction circle centered on its 2MASS

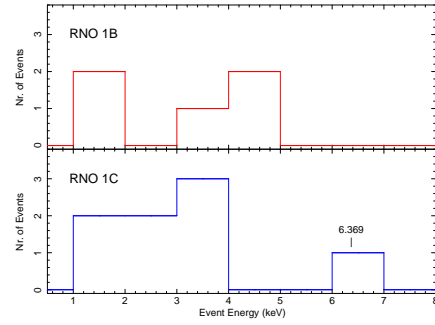


Figure 2. X-ray event energy histograms for RNO 1B/1C using energy bin widths of 1 keV.

position (2MASS J00364599+6328529). Three events were detected in the first observation and two in the second with energies in the range $E = 1.39$ - 4.75 keV and mean energy $\bar{E} = 3.09 \pm 1.40$ keV. For RNO 1C (2MASS J00364659+6328574), a similar extraction yielded 8 events, with four detected in each observation and a range $E = 1.45$ - 6.37 keV and $\bar{E} = 3.28 \pm 1.39$ keV. Its X-ray centroid lies $0''.7$ west of the radio source VLA 1 (J003646.67+632853.7; Anglada et al. 1994). Background is negligible (<1 count within $r=1''.5$ extraction regions).

Event energy distributions are plotted as histograms in Figure 2. The outlier event at 6.37 keV for RNO 1C is noteworthy since it may be due to fluorescent Fe produced when cold gas near the star is irradiated by hard X-rays, as has been detected in FU Ori itself (Skinner et al. 2006). But a spectrum of RNO 1C with more counts is needed to determine if fluorescent Fe emission near 6.4 keV is actually present.

We fitted the unbinned RNO 1C spectra with a simple absorbed single temperature thermal plasma model (1T APEC) using the C-statistic. Since the two spectra together provide only 8 counts, they do not reliably constrain the absorption column density N_H . It was thus stepped through values in the range $N_H = (1.7 - 4.5) \times 10^{22} \text{ cm}^{-2}$, corresponding to $A_V \approx 9 - 24$ mag in order to span previous extinction estimates. We adopt the conversion $N_H = 1.9 \times 10^{21} A_V \text{ cm}^{-2}$ obtained by averaging the slightly different conversions of Gorenstein (1975) and Vuong et al. (2003). The fits gave observed (absorbed) fluxes $F_{x,abs}(0.3-8 \text{ keV}) = 2.50(\pm 0.20) \times 10^{-15} \text{ ergs cm}^{-2} \text{ s}^{-1}$. The derived plasma temperature, unabsorbed flux, and intrinsic X-ray luminosity (L_x) are sensitive to the assumed value of N_H . The C-statistic is minimized for $N_H = (2.4 - 2.6) \times 10^{22} \text{ cm}^{-2}$ ($A_V \approx 12.6 - 13.7$ mag) and $kT \approx 3.2 - 3.7$ keV. The luminosity estimate is $\log L_x(0.3-8 \text{ keV}) = 29.83(\pm 0.15) \text{ ergs s}^{-1}$.

¹ Details on *Chandra* instrumentation and performance can be found in the *Proposer's Observatory Guide* at cxc.harvard.edu/proposer/POG.

Table 1. Chandra X-Ray Sources Near RNO 1B/C

Chandra position	Name	Net Counts	\bar{E} (E_{50})	Hardness	$F_{x,abs}$	$\log L_x$	Offset
R.A., decl. (J2000)		(cts)	(keV)		(ergs cm ⁻² s ⁻¹)	(ergs s ⁻¹)	(arcsec)
J00 36 46.04+63 28 52.8	RNO 1B	5±2	3.08 (3.09)	0.60	1.60(±0.20)e-15 ^b	29.64 ^b	0.34
J00 36 46.55+63 28 57.3	RNO 1C	8±3	3.28 (3.21)	0.75	2.50(±0.20)e-15 ^c	29.83 ^c	0.31
J00 36 47.12+63 28 50.1	RNO 1G	9±3	4.71 (4.59)	1.00	5.83(±0.20)e-15	30.41	0.22
J00 36 47.41+63 29 02.7	VLA 3	4±2	5.42 (5.36)	1.00	... ^d	... ^d	0.52
J00 36 47.30+63 28 56.1	anon	10±3	4.58 (3.85)	1.00	9.88(±0.62)e-15 ^e	31.04	...

^a Notes: Data are based on merged events (0.3 - 7 keV) from *Chandra* ObsIds 20135 and 21041, with a total livetime of 59.143 ks. Tabulated quantities are: J2000.0 X-ray centroid position (R.A., decl.); object name; net counts and net counts error; mean (\bar{E}) and median (E_{50}) event energies; Hardness = counts(2-7 keV)/counts(0.3-7 keV); absorbed X-ray flux (0.3-7 keV); unabsorbed X-ray luminosity at an assumed distance of 930 pc, and offset between *Chandra* and IR or VLA radio positions.

^b F_x and L_x are estimated from 1T APEC PIMMS simulations assuming absorption $N_H = (1.7 - 3.0) \times 10^{22}$ cm⁻² and kT = 3.0 - 5.4 keV.

^c F_x and L_x are estimated from 1T APEC fits of unbinned spectra assuming $N_H = (1.7 - 4.5) \times 10^{22}$ cm⁻².

^d Insufficient counts to determine F_x and L_x .

^e F_x is based on a 1T APEC fits of unbinned spectra with $N_H = (1-2) \times 10^{23}$ cm⁻² and kT = 1.6 - 4.1 keV.

Since only 5 counts were detected for RNO 1B we did not attempt spectral fits. Instead, we used the Portable Interactive Multi-Mission Simulator (PIMMS) to estimate the flux and L_x based on the ACIS-I count rate of 0.0845 c ks⁻¹. A 1T APEC absorbed thermal plasma model was used, as for RNO 1C. The absorption was stepped through values in the range $N_H = (1.7 - 3.0) \times 10^{22}$ cm⁻², corresponding $A_v \approx 9 - 16$ mag (Staude & Neckel 1991; CR18). We used two different plasma temperatures kT = 3 and 5.4 keV, typical of

FUors and classical (accreting) T Tauri stars. For the above range of values, PIMMS predicts $F_{x,abs}(0.3-8 \text{ keV}) = 1.60(\pm 0.20) \times 10^{-15}$ ergs cm⁻² s⁻¹ and unabsorbed luminosity $\log L_x(0.3-8 \text{ keV}) = 29.64(\pm 0.15)$ ergs s⁻¹. We emphasize that this L_x estimate is based on assumed values of N_H and kT that lie within reasonable ranges, but are not actual measurements. If N_H is greater than assumed (as could occur from cold gas along the line-of-sight that is not accounted for by A_v) or if kT is less, then higher L_x values are possible.

3.2. Other X-ray Sources Near RNO 1B/1C

CXO J003647.1+632850.1 is a 9-count X-ray source whose position is nearly coincident with the infrared source RNO 1G (J003647.14+632849.95; Quanz et al. 2007). RNO 1G is a deeply embedded young stellar object (YSO) originally identified in near-IR polarization maps by Weintraub & Kastner (1993). Both the X-ray and IR positions of RNO 1G are offset by $\approx 0''.5$ SE of radio continuum source VLA 2 (Anglada et al. 1994). The X-ray source is hard with event energies in the range $E = 3.46 - 6.19$ keV. Fits of the unbinned spectra with a 1T APEC model give a minimum C-statistic for

$N_H = (1.5 - 2.0) \times 10^{23}$ cm⁻², corresponding to $A_v \gtrsim 79$ mag, and high plasma temperatures kT $\approx 13 - 14$ keV.

CXO J003647.4+632902.7 is a faint source offset $\approx 0''.5$ NE of the 3.6 cm radio continuum source VLA 3. The radio source shows elongated structure and has a positive spectral index (Anglada et al. 1994), as commonly observed for driving sources of bipolar outflows. It was thus proposed by Anglada et al. that VLA 3 drives the bipolar molecular outflow in L1287 that was studied in millimeter molecular lines by Yang et al. (1991). There is no cataloged 2MASS source within $1''$ of the X-ray position but IRAS 00338+6312 lies $\approx 0''.9$ SE of the X-ray centroid. Four events were detected, of which 3 were detected in the first observation. The source is very hard with event energies in the range $E = 4.36 -$

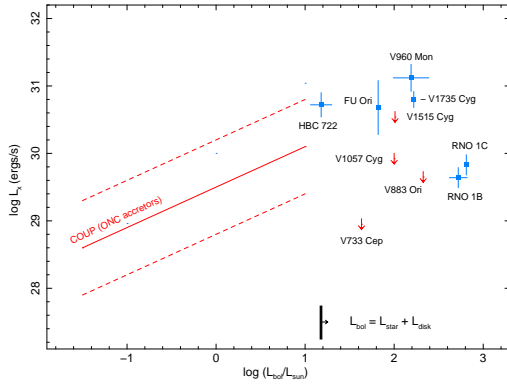


Figure 3. X-ray luminosity (L_x) versus bolometric luminosity (L_{bol}/L_\odot) for FUors observed by *Chandra* and *XMM-Newton* based on published and archival data. Downward arrows show upper limits for three FUors undetected by *XMM-Newton* (V1515 Cyg, V1057 Cyg, V883 Ori) and for the *Chandra* non-detection of V733 Cep. The regression fit for accreting sources in the Orion Nebula Cluster (ONC) are shown (red solid line) along with the ± 0.7 dex (1σ) dispersion in $\log L_x$ (red dashed line; Preibisch et al. 2005). The high L_{bol} values of FUors are dominated by the luminous accretion disk.

6.60 keV. The *Chandra* X-ray position may point to a deeply embedded (proto)star associated with the jet-like source VLA 3.

CXO J003647.3+632856.1 is a variable source which remarkably was only detected in the second *Chandra* observation (10 counts). This source is labeled “anon” in Figure 1. There is no catalogued 2MASS counterpart. The radio source VLA 4 (J003647.39+632853.7) lies $2''.3$ to the south. The X-ray source is hard with event energies $E = 2.93 - 6.82$ keV. Three events have energies $E = 6.36 - 6.82$ keV, suggestive of Fe emission. This object is likely a heavily embedded magnetically active (flaring) young star or protostar that is only intermittently detected in X-rays. We fitted the unbinned spectrum with a 1T APEC model. No *a priori* information on A_v is available but we assumed high X-ray absorption and stepped through values $N_H = (1 - 40) \times 10^{22} \text{ cm}^{-2}$. The C-statistic is minimized for $N_H = (1-2) \times 10^{23} \text{ cm}^{-2}$ ($A_v \gtrsim 52$ mag) with $kT \approx 2-4$ keV.

Non-Detections We find no significant X-ray emission at the position of the source tentatively identified as RNO 1D by Weintraub et al. (1996) or at the position of RNO 1F (Quanz et al. 2007).

4. DISCUSSION

4.1. RNO 1B and 1C in Context

The *Chandra* data show similar X-ray properties for RNO 1B and 1C. There is no significant difference in the number of events detected for the two stars or in

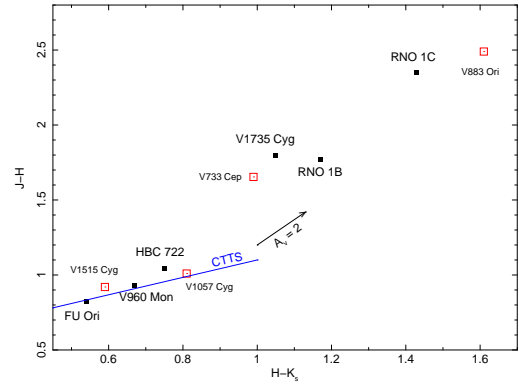


Figure 4. 2MASS near-IR colors for selected FUors observed by *Chandra* and *XMM-Newton*. Solid squares are X-ray detections and open squares are non-detections (see Fig. 3). The solid line showing *unreddened* colors for classical T Tauri stars and the reddening vector for $A_v = 2$ mag are based on Meyer et al. (1997).

their mean event energies to within the uncertainties. Spectra with a larger number of counts will be needed to determine if real differences exist. Since no pre-outburst X-ray spectra are available for RNO 1B (or for FUors in general) we do not know whether its X-ray properties were affected by the 1978 - 1990 eruption.

Our L_x estimates for RNO 1B and 1C make them the least X-ray luminous FUors detected to date, about a factor of ten less luminous than the X-ray bright sources FU Ori ($\log L_x = 30.68 \text{ ergs s}^{-1}$), V1735 Cyg ($\log L_x = 30.80$), and V960 Mon ($\log L_x = 31.12$). The faint X-ray emitting FUor-like source L1551 IRS 5 has a lower L_x than RNO 1B and 1C but its X-ray emission is offset from the obscured central object and probably originates in its jet (Favata et al. 2002; Bally et al. 2003; Schneider, Günther, & Schmitt 2011). Upper limits for a few undetected FUors are comparable to or less than the L_x values of RNO 1B and 1C. For example, V883 Ori was undetected by *XMM-Newton* at $\log L_x \leq 29.65 \text{ ergs s}^{-1}$ (ObsId 0205150501; PI: S. Skinner). Also, three archived *Chandra* ACIS-I exposures with a combined livetime of 71.675 ks (ObsIds 9919, 10811, 10812; PI: T. Allen) captured V733 Cep far off-axis but it was not detected. This star erupted in 1971 or earlier and has optical and near-IR spectra very similar to FU Ori (CR18). Based on all three *Chandra* exposures, we obtain a conservative upper limit $\log L_x(0.3-8 \text{ keV}) \leq 28.95 \text{ ergs s}^{-1}$ at $d = 800 \text{ pc}$ (CR18) assuming a thermal plasma spectrum with $kT = 3 \text{ keV}$ and extinction as large as $A_v = 11.5 \pm 1 \text{ mag}$ (CR18), equivalent to $N_H \approx 2.2 \times 10^{22} \text{ cm}^{-2}$. If the *Gaia* DR2 distance of $669^{+50}_{-43} \text{ pc}$ for V733 Cep is adopted then a more stringent upper limit $\log L_x(0.3-8 \text{ keV}) \leq 28.80 \text{ ergs s}^{-1}$ is obtained. The derived upper limits are sensitive to the assumed values of

N_H and kT . If the actual N_H is higher or kT lower than assumed above, then the upper limits increase. Despite its spectroscopic similarity to FU Ori, it is much fainter in X-rays and so far undetected down to rather stringent upper limits.

As shown in Figure 3, the X-ray luminosities of RNO 1B and 1C are comparable to accreting classical T Tauri stars (Preibisch et al. 2005; Telleschi et al. 2007) despite the fact that FUors have much higher bolometric luminosities. At our assumed distance of 930 pc, the results of Gramajo et al. (2014) give $L_{bol} = 527 L_\odot$ (RNO 1B) and $646 L_\odot$ (RNO 1C). These L_{bol} values are quite high, even for FUors (CR18). It is thus clear that high L_{bol} for FUors does not necessarily translate into high L_x . By comparison, a general trend for an increase in L_x with L_{bol} is seen in classical T Tauri stars, albeit with large scatter in L_x (Fig. 3). Since L_{bol} in FUors is dominated by a luminous accretion disk, any possible dependence of L_x on the luminosity of the central star (L_*) will be difficult to establish without reliable estimates of L_* .

Similarly, a correlation with stellar mass $L_x \propto M_*$ exists for classical T Tauri stars (Preibisch et al. 2005; Telleschi et al. 2007), but no such correlation has yet been established for FUors since their stellar masses are not well known. There is even disagreement as to whether the prototype FU Ori is a subsolar mass star (Zhu et al. 2007) or a more massive object (Herbig et al. 2003). But in a few cases, pre-outburst optical and near-IR observations show that the progenitor was a young late-type star. For example, HBC 722 (= LkH α 188-G4 = V2493 Cyg) was classified as a K7-M0 star by Cohen & Kuhl (1979), implying a subsolar mass progenitor.

4.2. Comments on FUor X-ray Emission

Since some FUors are detected as luminous X-ray sources whereas others are undetected down to rather stringent upper limits (e.g. V733 Cep), we would like to know what factor(s) ultimately govern their X-ray properties. Since the stars themselves are generally heavily-obscured, we lack sufficient data about stellar properties (e.g. mass, stellar luminosity, rotation period, magnetic field strength, accretion rate) to answer this question. However, their bolometric luminosities have been determined and as noted above the $L_x \propto L_{bol}$ relation seen in classical T Tauri stars does not hold for FUors.

Previous observations show that the *detected* X-ray emission of FUors cannot be due entirely to accretion shocks. Even though their accretion rates are as high as $\dot{M}_{acc} \gtrsim 10^{-5} M_\odot \text{ yr}^{-1}$ during outbursts, accretion shock emission is expected to produce only cooler X-ray plasma at characteristic temperatures $T_{shock} \sim 1 - 2$ MK ($kT_{shock} \sim 0.1 - 0.2$ keV) for plausible infall speeds

of a few hundred km s^{-1} (Skinner et al. 2009). A similar conclusion holds for shocked winds or jets assuming terminal speeds of a few hundred km s^{-1} (Raga et al. 2002). However, it is worth noting that soft accretion shock emission from very cool plasma would be difficult to detect when viewed through the high absorption of some FUors. Such objects include RNO 1C whose near-IR colors (Fig. 4) and high A_V estimates (Sec. 1) indicate heavy reddening. Furthermore, additional X-ray absorption from dust-depleted gas that is not accounted for by A_V may be present. This is probably the case for FU Ori which shows X-ray evidence for cold gas near the star in the form of fluorescent Fe I X-ray emission (Skinner et al. 2006). Another example is HBC 722 which showed apparently variable circumstellar X-ray absorption by dust-depleted gas in early outburst (Liebhart et al. 2016).

Even though the hot X-ray plasma detected in FUors cannot be attributed to accretion shocks, FUor X-ray properties might be affected by accretion. This could occur if enhanced accretion during optical/IR outbursts alters the magnetic field topology or stellar structure, as has been suggested for accreting T Tauri stars (Preibisch et al. 2005) and the eruptive young star V1118 Ori (Audard et al. 2010).

Fits of the X-ray component detected in FUors with thermal plasma models typically give $kT \gtrsim 3$ keV ($T \gtrsim 35$ MK). Our fits of the low-count RNO 1C *Chandra* spectrum are consistent with such high temperatures. In the case of FU Ori, the X-ray count rate in the hard 2-8 keV band varied on a timescale of less than one day (Skinner et al. 2010). Such variable hard emission clearly points to magnetically-controlled processes. The cause of the variability is not known, but the <1-day timescale is suggestive of magnetic-reconnection flares. Even so, the factor of ~ 2 variability in the hard-band count rate of FU Ori is rather modest compared to the powerful impulsive X-ray flares that have been detected in some T Tauri stars and class I protostars.

X-ray monitoring of FUors in the time domain is still quite limited. Long-term X-ray monitoring is needed to search for powerful impulsive X-ray flares and for evidence of periodic or quasi-periodic emission. Periodic emission could be induced by stellar rotation and would provide insight into poorly-known rotation periods, as has been demonstrated for the protostar V1647 Ori (Hamaguchi et al. 2012). Orbital X-ray modulation could also be present if some FUors are close binaries, as suggested by Reipurth & Aspin (2004).

5. SUMMARY

Chandra observations of the close pair of similar FUor-like stars RNO 1B and 1C reveal faint X-ray emission with intrinsic luminosities $\log L_x = 29.64 - 29.83$ ergs s^{-1} , making them the faintest X-ray detections among FUors to date. Their low L_x in combination with high L_{bol} shows that the $L_x \propto L_{bol}$ relation present in classical T Tauri stars does not carry over to FUors. Their X-ray spectral properties are not well-constrained due to the low number of detected counts but our analysis suggests high plasma temperatures $kT \gtrsim 3$ keV and high absorption $N_H \gtrsim 10^{22}$ cm $^{-2}$, the latter being consistent with existing A_v estimates. The high plasma temperature

implies that the detected X-ray emission is due to magnetic processes, not accretion shocks or shocked winds.

Support for this work was provided by *Chandra* X-ray Center award GO 8-19004X.

Facilities: Chandra(ACIS)

Software: CIAO (Fruscione et al. 2006), XSPEC (Arnaud 1996)

REFERENCES

- Anglada, G., Rodríguez, L.F., Girart, J., Estalella, R., & Torrelles, J.M. 1994, *ApJ*, 420, L91
- Arnaud, K.A. 1996, in ASP Conf. Series vol. 101, *Astronomical Data Analysis Software and Systems V*, ed. G. Jacoby & J. Barnes (San Francisco, CA; ASP), 17
- Audard, M., Ábrahám, P., Dunham, M.M. et al. 2014, in *Protostars and Planets VI*, eds. H. Beuther et al. (Tucson, AZ: Univ. of Arizona Press), 387
- Audard, M., Stringfellow, G.S., Güdel, M. et al. 2010, *A&A*, 511, A63
- Bally, J., Feigelson, E., & Reipurth, B. 2003, *ApJ*, 584, 843
- Cohen, M. 1980, *AJ*, 85, 29
- Cohen, M. & Kuhl, L.V. 1979, *ApJS*, 41, 743
- Connelley, M.S. & Reipurth, B. 2018, *ApJ*, 861, 145 (CR18)
- Favata, F., Fridlund, C.V.M., Micela, G., Sciortino, S., & Kaas, A.A. 2002, *A&A*, 386, 204
- Fruscione, A., McDowell, J.C., Allen, G.E. et al. 2006, *Proc. SPIE*, 6270, 62701V
- Gramajo, L.V., Rodón, J.A., & Gómez, M. 2014, *AJ*, 147, 140
- Hamaguchi, K., Grosso, N., Kastner, J.H., Weintraub, D.A., Richmond, M., Petre, R., Teets, W.K., & Principe, D. 2012, *ApJ*, 754, 32
- Herbig, G.H., Petrov, P.P., & Duemmler, R. 2003, *ApJ*, 595, 384
- Kenyon, S.J., Hartmann, L., Gomez, M., Carr, J.S., & Tokunaga, A. 1993, *AJ*, 105, 1505
- Liebhart, A., Güdel, M., Skinner, S.L., & Green, J. 2014, *A&A*, 570, L11
- Meyer, M.R., Calvet, N., & Hillenbrand, L.A. 1997, *AJ*, 114, 288
- Preibisch, T., Kim, Y.-C., Favata, F. et al. 2005, *ApJS*, 160, 401
- Quanz, S.P., Henning, Th., Bouwman, J., Linz, H., & Lahuis, F. 2007, *ApJ*, 658, 487
- Raga, A.C., Noriega-Crespo, A., & Velázquez, P.F. 2002, *ApJ*, 576, L149
- Reid, M.J., Menten, K.M., Brunthaler, A. et al. 2014, *ApJ*, 783, 130
- Reipurth, B. & Aspin, C. 2004, *ApJ*, 608, L65
- Schneider, P.C., Günther, H.M., & Schmitt, J.H.M.M. 2011, *A&A*, 530, A123
- Skinner, S.L., Briggs, K.R., & Güdel, M. 2006, *ApJ*, 643, 995
- Skinner, S.L., Güdel, M., Briggs, K.R., & Lamzin, S.A. 2010, *ApJ*, 722, 1654
- Skinner, S.L., Sokal, K.R., Güdel, M., & Briggs, K.R. 2009, *ApJ*, 696, 766
- Staude, H.J. & Neckel, Th. 1991, *A&A*, 244, L13 (SN91)
- Telleschi, A., Güdel, M., Briggs, K.R., Audard, M., & Palla, F. 2007, *A&A*, 468, 425
- Weintraub, D.A. & Kastner, J. 1993, *ApJ*, 411, 767
- Weintraub, D.A., Kastner, J., Gatley, I., & Merrill, K.M. 1996, *ApJ*, 468, L45
- Yang, J., Umemoto, T., Iwata, T., & Fukui, Y. 1991, *ApJ*, 373, 137
- Zhu, Z., Hartmann, L., Calvet, N., Hernandez, J., Muzerolle, J., & Tannirkulam, A.-K. 2007, *ApJ*, 669, 483